energies

MDPI

Article

Linear Programming-Based Power Management for a Multi-Feeder Ultra-Fast DC Charging Station

Luigi Rubino [1,*,†], Guido Rubino [2,†] and Raffaele Esempio [1,†]

[1] Department of Engineering, University of Campania Luigi Vanvitelli, 81031 Aversa, CE, Italy
[2] Department of Electrical and Information Engineering (DIEI), University of Cassino and South Lazio, 03043 Cassino, FR, Italy
* Correspondence: luigi.rubino@unicampania.it; Tel.: +39-081-5010317
† These authors contributed equally to this work.

Abstract: The growing number of electric vehicles (EVs) affects the national electricity system in terms of power demand and load variation. Turning our attention to Italy, the number of vehicles on the road is 39 million; this represents a major challenge, as they will need to be recharged constantly when the transition to electric technology is complete. If we consider that the average power is 55 GW and the installed system can produce 120 GW of peak power, we can calculate that with only 5% of vehicles in recharging mode, the power demand increases to 126 GW, which is approximately 140% of installed power. The integration of renewable energy sources will help the grid, but this solution is less useful for handling large load variations that negatively affect the grid. In addition, some vehicles committed to public utility must have a reduced stop time and can be considered to have higher priority. The introduction of priorities implies that the power absorption limit cannot be easily introduced by limiting the number of charging vehicles, but rather by computing the power flow that respects constraints and integrates renewable and local storage power contributions. The problem formulated in this manner does not have a unique solution; in this study, the linear programming method is used to optimise renewable resources, local storage, and EVs to mitigate their effects on the grid. Simulations are performed to verify the proposed method.

Keywords: ultra-fast charging; electric vehicles (EVs); power management (PM); grid-connected converters

Citation: Rubino, L.; Rubino, G.; Esempio, R. Linear Programming-Based Power Management for a Multi-Feeder Ultra-Fast DC Charging Station. *Energies* **2023**, *16*, 1213. https://doi.org/10.3390/en16031213

Academic Editor: Giovanni Lutzemberger

Received: 21 December 2022
Revised: 11 January 2023
Accepted: 17 January 2023
Published: 22 January 2023

1. Introduction

Recently, *So*Cial, economic, and environmental factors sustained by government policies have increased interest in and support for the electrification of transportation [1,2]. In this context, most major car manufacturers have proposed new electric vehicles (EVs) and plug-in hybrid electric vehicles (PHEVs) that can reduce greenhouse gas emissions by phasing out all combustion vehicles [3]. Renewable sources affect power grid stability, owing to intermittent production, and by increasing the installed renewable power sources, negative effects will further increase [4]. Therefore, electricity companies are investing in large amounts of energy storage to stabilize the grid. For example, in Italy, the national electric power transmission *So*Ciety TERNA built an experimental storage plant that is physically distributed throughout the territory, reaching a total of 10 MW [5]. Currently, the most effective techniques with a reduced impact on the electricity grid are local generation from renewable sources using an energy storage system [6,7]. Based on this idea, some countries, such as Italy, encourage photovoltaic installation for residences with the addition of local storage [8,9]. It must also be considered that the increase in electric vehicles compared to the past brings a new problem; the high demand for electrical power during grid-to-vehicle (G2V) simultaneous charging can be higher than the power grid's capability, leading to grid instability [10–14]. In [12], the load-shifting method was indicated as a possible solution to grid overload, owing to power peak shaving and power valley filling. In other words, by distributing power absorption during the day, the grid's power can be averaged, resulting

in a more stable system. A different approach is based on the idea that EVs can also be used for large energy storage systems when the grid is overloaded. When individual vehicles or public and private transport fleets are stopped, batteries can be recharged flexibly or used to feed energy into the grid, thus ensuring better management of electricity demand peaks (load shifting and peak shaving). Based on this concept, vehicle-to-grid (V2G) technology uses a bidirectional charger and actively controls the power of electric vehicles [15]. Both approaches only solve the problem when EVs are connected to the grid for a long time, for instance, at night or during working hours. In addition to V2G, power exchange can be generalized by introducing vehicle-to-everything (V2X) technology, which locally limits the drawbacks of loads and EVs on the grid [16].

All these techniques require charging stations for EVs to be intelligent [17]; that is, in addition to charging a car, they must have software and communication protocols for state estimation and energy-management integration. In this paper, we refer to ISO/IEC 15118, the Open Charge Point Protocol and IEC 61850 for the communication rules between the charging station and the grid for V2G [18–20]. We refer to IEC 61851 for the communication system between the charging station and EV [21]. Other relevant problems, which are not discussed in this work, are related to smart metering and data privacy preservation [22], packet length definition [23] and network security [24]. From a software perspective, energy management has several objectives. Therefore, the supervision logic for the G2V and V2X operations must define the charge/discharge power for each instant of time for the connected EVs. As inputs, it considers the grid status, renewable energy production, and EV parameters, such as the *SoC*, maximum charging current, economic conditions, and other parameters. In [25], an example of a multi-objective optimization method for G2V and V2G was presented. Additional constraints may be minimization of the purchase costs of electricity and calculation of whether to use a renewable source or an accumulation source, maximizing its useful life [26]. Optimization can also be improved by considering the prediction of energy production from renewable sources, as studied in [27,28]. Notably, some already marked charging stations are ready for this type of technology. Among the EV charging solutions equipped with energy management, several companies avoid excessive demand for grid power, offering standalone or energy rationalization systems. The ABB offers an electric vehicle management system (load management). The management of electric vehicles can be carried out according to FIFO logic (first in first out) or equal share [29], but they plan to launch V2G technology on the market soon. Delta Electronics proposed DeltaGrid EVM [30], which integrates a storage system from renewable sources (such as photovoltaics) to reduce peaks in electricity demand and prevent overloads from exploiting the existing energy in the infrastructure. The Shell Company provides energy-management solutions for large charging stations [31]. Stations can integrate storage systems and renewable generation systems, but do not specify how the loads and generators are managed. All these solutions have power limits imposed by the network, and as a result, strategies are being implemented in many countries to stabilize the grid. In Italy, the electricity company TERNA [32,33] has issued an important ten-year investment plan for the challenges posed by the EV ecological transition, and in particular for V2G and G2V technologies, which have the opportunity to participate in the dispatching service market as they are completely comparable to archiving systems. In the literature, supervisor methods can be divided into two groups: (i) centralized and (ii) decentralized optimization models. The first approach is better in terms of solution accuracy because of the detailed knowledge of system state variables [34]. The decentralized approach wins when the system under optimization is distributed over a large geographical area, because of its ability to work with reduced communication between systems [35].

To the best of the authors' knowledge, the charging stations in the literature do not distinguish differences among vehicles, because the optimisation typically considers the CO_2 emissions and power limits but not the type of a vehicle. Consequently, emergency vehicles (EMVs) (e.g., ambulances, police, and firefighters) must respect the charging order. The scope of this study is to overtake rigid charging-order scheduling and reformulate the

energy-management problem by adding priorities to the constraints (e.g., power limits). Each electric vehicle is associated with a different priority, and the vehicles with the highest priority can absorb power up to the limit. Furthermore, the method not only schedules the charging time for each vehicle, but also defines the charging power level and, in the case of a grid overload, the discharging power level. The motivation for this study is based on the idea that by increasing the number of electrical vehicles, the available power decreases, and depending on the hour of the day, the charging time spreads to levels that are not acceptable for the EMVs. This paper proposes a possible solution to this problem. In addition, most scientific work on charging stations focuses on low/medium-power urban charging stations with electric vehicles connected for hours, which are generally directly connected to the grid. This study examined different ultrafast charging stations designed for motorways, where the charging time is critical and the scheduling logic must be carefully considered. The proposed ultrafast charging station (UFCS) integrates local storage and renewable energy sources, which is not common in urban UFCSs.

The contributions of this study can be summarized as follows:

- Creation a simulation model of an ultra-fast DC charging station for motorways. The model includes grid loads that are statistically defined from the data provided by TERNA. Moreover, the model simulates different types of charging vehicles, each defined from a set of stochastically generated parameters, such as battery capacitance, *SoC*, peak power for charging/discharging, arrival time, and priority number;
- Implementation of a centralized optimization software, based on a Linear Programming method, to manage the power exchange between the EV sources and the grid;
- Development of simulation software to test logic, better described below;
- Verification by simulation that the constraints are respected.

It should be noted that the centralized approach for the proposed charging station is not limited, as each UFCS can be seen by the network as a single [36]. In this study, for modeling, we assumed that the state of the grid is measurable and known to the UFCS. Finally, through a simulation, we verified that the proposed method respects the concepts of peak shaving and valley filling, thus helping the grid despite the considered installed power of the UFCS being 3 MW.

2. Proposed Ultra Fast Charging Station for Motorways

This section reports the proposed UFCS with the rules and modelling used for the simulations. It is conceptually composed of three parts. In the first part, the UFCS is detailed in terms of all the relevant aspects. In the second part, a statement on the optimisation problem for UFCS supervision is introduced. The simulation structure is reported. The power flow supervisor proposed for the ultrafast charging station manages vehicles according to the priority assigned to each of them. This implies that EVs are scheduled to charge or discharge, depending on the priority assigned. The highest priority electric vehicles EMVs have confidential contracts, are not usable in the V2X operating mode and are loaded to the maximum allowed power by skipping the queue order. The other loads must respect the queue order defined by the priority and arrival times.

The UFCS topology considered is reported in Figure 1 [15]. It is composed of an internal DC voltage bus connected to a renewable photovoltaic power source and uses battery energy storage (BESS) for peak shaving. Finally, the UFCS was connected to the grid. Owing to the presence of power converters for each element of the UFCS and grid connection, the power flow can be independently controlled by the UFCS supervisor. It should be noted that the type of renewable power source does not affect the proposed method and can be integrated with other sources such as wind energy and wave energy. There are similar considerations for local energy storage. The UFCS can also integrate a flywheel or other types of storage to help the grid, without a lack of generality [37].

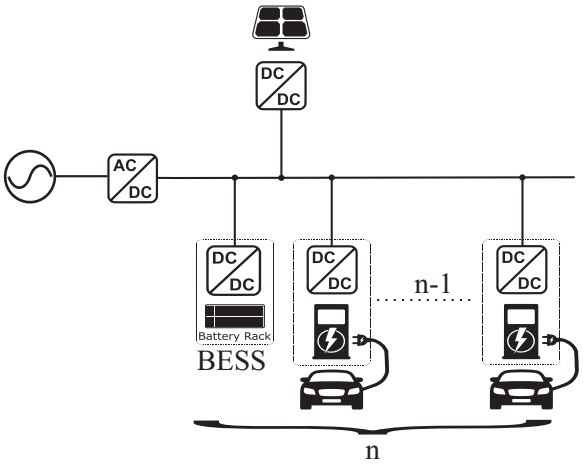

Figure 1. High-level view of the charging station structure composed of n storages with different priority.

The priorities of EVs were calculated according to certain parameters. The most important parameters are the type of contract, desired charging time, and discount on the negotiated energy price.

The EV priority increases over time to the maximum priority level associated with the class of thr contracts. Because the priorities are partially related to the market and policies, without a lack of generalities, we assume in this study that the priorities are externally assigned (randomly generated), limiting the study's contribution to the methods to manage them for the UFCS.

Moving to a higher level, we can model the UFCS by considering grid integration and communication protocols, as shown in Figure 2. This scheme starts from the idea proposed in [38], but differs in the introduction of the priorities and the integration of the BESS and renewable energy at the UFCS nanogrid level. The EV service provider captures the user agreement, scheduled arrival time, and departure time and provides priority level ξ_i and the minimum allowed SoC during V2X for the ith EV. The remaining data required to clearly define the problem are acquired directly from the EV through the communication system of the EV power equipment. The vehicle parameters are the SoC, the maximum allowed power for charging P_i^{G2V}, and the maximum discharging power P_i^{V2X}. These parameters are generally runtime-estimated onboard the EV, ensuring the safety of the charging or discharging operations [39] in the case of variations in cell parameters [40], or limiting power in the case of bad current split among cells in parallel [41]. Finally, the collected data were sent to the UFCS power flow supervisor.

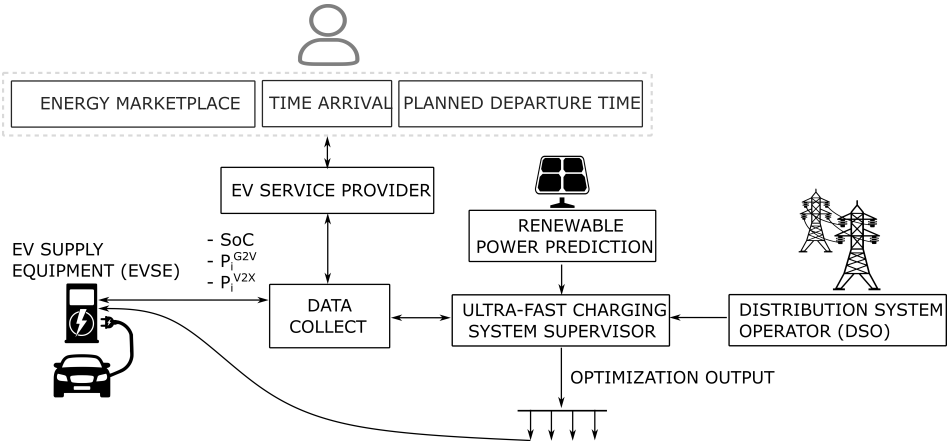

Figure 2. Fast charging integration with the grid.

Similar parameters are acquired from the BESS, except that the priority automatically changes depending on the type of connected EV. When one or more EMVs are refilling, we prefer to use the energy stored in the BESS to help the grid and reduce the charging time. This rule can be expressed as the switching function of (1), where n_{EM} is the number of refilling EMVs and ξ_{b0}, ξ_{b1} are the defined priorities, respectively, in the case of one or more charging EMVs or no emergency vehicles at the UFCS. This position reduces the EVs contribution to V2X when no EMVs are connected.

$$\xi_{bess}^{V2X} = \xi_{b0}(n_{EM} > 0) + \xi_{b1}(n_{EM} == 0) \tag{1}$$

$$P_{bess}^{G2V} = \begin{cases} P_{bessMAX}^{G2V}\left(1 - \frac{1}{80-a_{bess}}(SoC_{bess} - a_{bess})\right) & \text{if } (SoC_{bess} \geq a_{bess}) \\ P_{bessMAX}^{G2V} & \text{else} \end{cases} \tag{2}$$

Figure 3 shows the power limits for the BESS and EVs as a function of the *SoC*. Each system can be charged or discharged at a power level depending on the vehicle. For simplicity, the power value was assumed to be constant. The first in Figure 3 is for the G2V operating mode. EVs can be ideally charged at a fixed power until the *SoC* reaches 80%; then, the vehicle is disconnected and a new EV can be connected for refilling. A different approach was adopted for the BESS. It is charged to full power only when the *SoC* is below the threshold a_{bess}. The BESS charging power was linearly reduced after that point, assuming a zero value in the case of 80% *SoC*. Equation (2) reports the BESS charging power as function of the *SoC*. In the fourth quadrant of Figure 3, we have two thresholds, a_i and b, which are used to decide when to stop the V2X power contribution for the related EV_i or BESS storage. When the *SoC* is below this limit, the power contribution is zero; otherwise, it is equal to the maximum allowed by the depicted element.

With the rules defined in the figure, storage cannot be used for the V2X operating mode when *SoC* is below the assigned trigger level. It should be noted that the limits can be easily extended with different functions by adding other parameters, such as battery temperature, as inputs.

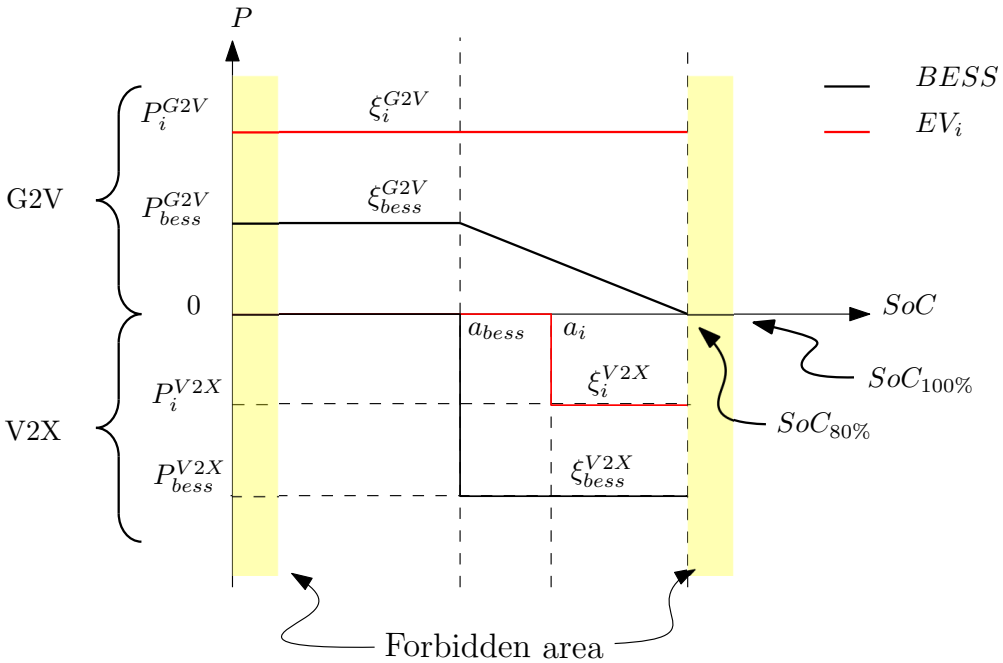

Figure 3. BESS and EV power level and priority as a function of *SoC*.

2.1. The Electrical Load Demand Modeling

The load curve $P_{ld}(LT)$ was generated from statistical data provided by TERNA [42] and is function of the local time (LT). By writing LT in terms of step time Δt, the $P_{ld}(LT)$ can be rewritten as (3).

$$P_{load}(k) = P_{ld}(k\Delta t) \tag{3}$$

The idea is that the shape of the load is repetitive during working days, and its peak value should not exceed 50% of the installed power. Starting from these assumptions, a load curve with time step Δt was sampled first, and then the curve was scaled for the case study.

2.2. Renewable Power Modeling

The simulation model included a photovoltaic (PV) power source. This choice is credible because PV is one of the most widely used renewable power sources in southern Italy, where the UFCS case study was installed [43]. The integration of other renewable energy sources does not lack generality. The power capability of a PV plant is a complex problem that has been extensively investigated by several authors. The maximum power produced depends, in its basic estimate, on the geographical coordinates, in particular on the latitude, the day of the year, the hour, the orientation of the PV panels, and the size of the plant in terms of the number of installed PV panels [44–46]. Weather forecasts can also be added to the model to predict the maximum extracted power better. The model does not consider PV shading or other non-idealities that can reduce the maximum power produced. With this assumption, the power depends on the position of the sun, which can be defined using Almanac software and sampled with step time Δt. In its basic form, the power output is calculated using (4) [47].

$$P_{PV}(k) = \mathrm{Y}\ \overrightarrow{u}_p \cdot \overrightarrow{\theta}(k) \tag{4}$$

The PV power $P_{PV}(k)$ is proportional to the scalar product of the vector perpendicular to the PV panel $\overrightarrow{u}_p$ and the position of the sun $\overrightarrow{\theta}(k)$. The constant Y includes all constants for the conversion of irradiation into power, as reported in [47].

2.3. Battery Modeling

For simplicity, the SoC of battery ith is calculated using the Coulomb method: first, the stored energy is calculated, and second, the result is obtained by dividing the energy by the battery capacity $Ebat_v$ [48]. For the runtime simulation, the forward Euler method was used for energy calculation. Moreover, the battery capacity $Ebat_v$ is included in the integration constant to estimate the SoC value directly, as in (5) [25].

$$SoC_i(k+1) = SoC_i(k) + \eta_{EV}\frac{P_i(k)\Delta t}{Ebat_i} \tag{5}$$

For simplicity, we assume $\eta_{EV} = 1$ for the simulations.

2.4. Proposed Linear Programming Optimization Method

The method has two main rules: it does not exceed the available power (6a), and it never discharges the EMVs (6b). The available power $P_{net} + P_{PV}$ is equal to the sum of the grid power capability P_{net} and the renewable power P_{PV} contribution, with P_{net} defined in (6c) as the difference between the installed power $P_{installed}$ and grid load power P_{load}. The element P_i^{EM} is the power demand of the ith EM vehicle and P_i^{EV} refers to the power

required for the ith EV. The remaining rules were introduced to comply with EV limits for electric vehicles.

$$P_{net}(k) + P_{PV}(k) \geq \sum_{i=1}^{n_{EM}} P_i^{EM}(k) + \sum_{i=1}^{n_{EV}} P_i^{EV}(k) \tag{6a}$$

$$\sum_{i=1}^{n_{EM}} P_i^{EM} \geq 0 \tag{6b}$$

$$P_{net}(k) = P_{installed} - P_{load}(k) \tag{6c}$$

Equation (6) indicates that the problem is linear with limits; for these reasons, the authors adopted a linear optimisation method for the solution, as explained in this subsection. Assuming that variables are functions of k, without a lack of generalities, the dependent variable is not reported hereafter.

The proposed power flow supervisor must know the state of the UFCS, the grid's available power and renewable power limits to define the power allocated to each storage. For the optimisation problem, we keep the models simple, as is common for this type of application [25]; this is because for a real UFCS, some inputs are directly measured or provided by an external control, and the uncertainty due to the reduced complexity of the models can be rejected using the measurements. On this basis, we assume that all converters are ideal with a unity efficiency. In this section, Figure 1 is referred to as the reference for the modelled blocks.

The G2V operating mode plays a major role in the charging stations. All input parameters were considered to be known or estimated using external software, and we assumed positive charging power during the G2V phase.

In Figure 1, n indicates the maximum number of storage units connected to the UFCS, including EVs and BESS. The working power of each element is defined by the UFCS supervisor described here, and for this operating mode, each element is defined by the priority number $\xi^\top = (\xi_1\ \xi_2\ ...\ \xi_n) \in \mathbb{N}^n$, positive integers. Note that ξ plays a key role in defining a strategy. If the priority increases linearly during the charging time, then the scheduling time behaves similarly to that of the FIFO method. A more complex scheduling method can be obtained by changing the maximum priority value assigned to each EV. In this study, for nonemergency vehicles, each EV had an initial priority that increased linearly over time and was limited to 90% of the priority scale. The EMVs had a fixed priority greater than 90%.

The peak allowed power is $P_{G2V}^\top = (P_1^{G2V}\ P_2^{G2V}\ ...\ P_n^{G2V}) \in \mathbb{R}_+^n$ positive real numbers, the assumed constant in this work as shown in Figure 3 and better described in Section 2. This input defines the maximum charging power and is generally defined by the EV. For a local storage BESS, this parameter is managed by the UFCS supervisor and changes depending on the SoC. It is zero when the BESS is charged and equal to the maximum charging power when under the threshold, as shown in Figure 3.

The V2X operating mode occurs when the grid is overcharged, or more specifically, when (6) is $false$. This event occurs when one or more EM vehicles are connected to the UFCS and the total available power from the grid and photovoltaic power is limited. In this case, the local BESS and remaining EVs are used as energy sources according to their capabilities, defined by the vector $P_{V2X}^\top = (P_1^{V2X}\ P_2^{V2X}\ ...\ P_n^{V2X}) \in \mathbb{R}_+^n$ positive real numbers.

The output is defined by vector $x^\top = (x_1\ x_2\ ...\ x_n) \in \mathbb{R}^n$, which corresponds to the power provided to the corresponding storage.

The linear programming problem maximizes the power assigned to storage units with higher priority by respecting constraints defined in terms of the maximum power level that can be absorbed by the sources and limits of each storage (7).

$$\max_{x} \quad \xi^{\top} x \tag{7a}$$

$$\text{subject to} \quad \sum_{i=1}^{n} x_i \leq P_{net} + P_{PV} \tag{7b}$$

$$-P_1^{V2X} \leq x_1 \leq P_1^{G2V} \tag{7c}$$

$$-P_2^{V2X} \leq x_2 \leq P_2^{G2V} \tag{7d}$$

$$\ldots \tag{7e}$$

$$-P_n^{V2X} \leq x_n \leq P_n^{G2V} \tag{7f}$$

(7a) ensures that the EVs with the highest priority are charged first and have a higher power level. It should be noted that if some elements have a low priority, a possible solution is obtained by assigning the element negative power. This is the key concept assumed in this study, having only one optimization problem for both the G2V and V2X operating modes. (7b) is (6a) rewritten for the linear programming optimization problem and introduced to limit the absorbed power to the grid's capability. The remaining equations, from (7c) to (7f), customize the problem for each EV. For EMVs, only positive solutions are accepted according to (6b) and the battery capability. For normal vehicles and BESS, the limits are defined as shown in Figure 3 and are better described in Section 2.

In the end, the proposed method was tested using a custom simulation algorithm developed with a script M-file in MATLAB. It is primarily composed of three sections, as shown in Figure 4, where

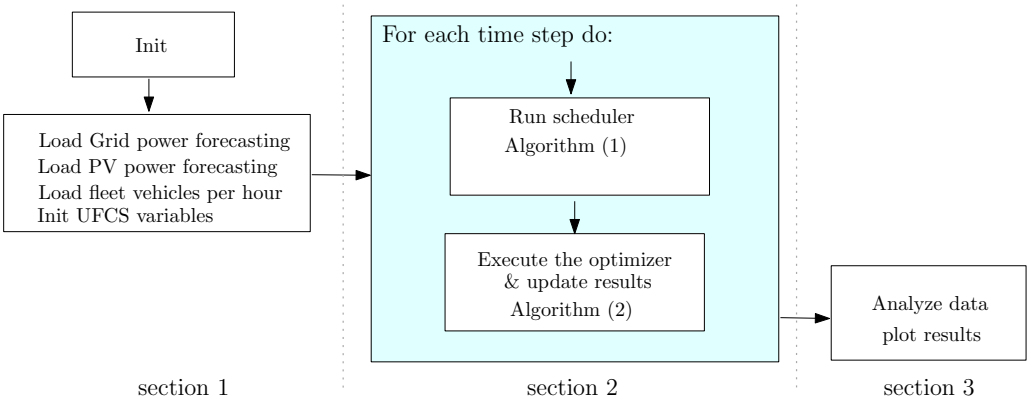

Figure 4. Structure of the developed simulator.

- First section: The first section is responsible for generating the statistical distribution of EVs, defining the initial *SoC*, and related maximum charging/discharging power. This section also defines the grid load profile P_{load} introduced above. Additional data are related to the PV power production P_{PV}. It should be noted that, with few changes, the simulation can be customized for different rules.
- Second section: The second section is the core of simulation software. It was composed of a loop cycle executed at every time step, Δt. At each cycle, first the scheduler Algorithm 1 is executed. It connects a new vehicle in case one or more EVSE are idle, and disconnects refilled vehicles. The scheduler is also in charge of the priorities update and the BESS' management in terms of priority and refilling power. For the simulation, we assume that arriving vehicles that find all the EVSE of the UFCS busy will go to the next UFCS, so no queues are considered in the case of this study.
  The next step is syntetically resumed in the Algorithm 2. It updates the input variables function of the step time as for the photovoltaic power and grid power. It executes the

optimization software defined in (7) and calculates the new *SoC* of storages. At the end, it updates the results.

- Third section: The third section is in charge only of the data analysis and plot of the results, as reported in the next section for a case study.

Algorithm 1: Pseudo-code of the scheduler.

Input: $n, \xi, EVSE, N_h, \xi_{b0}, \xi_{b1}, n_{EM}, SoC_i$
Result: $\xi, EVSE, N_h, n_{EM}$
/* the index $i = 1$ is reserved for the BESS. Start loop from 2 */
for $i = 2$ **to** n **do**
  if ($EVSE_i$ *available*) *AND* ($N_h > 0$) **then** /* connect a new vehicle */
    connect a new vehicle
    $EVSE_i \leftarrow$ busy ;
    $N_h \leftarrow N_h - 1$;
    if $\xi_i \geq \xi_{max}$ **then** /* update the number of EMVs */
      $n_{EM} \leftarrow n_{EM} + 1$
    end
  else
    if $\xi_i < \xi_{max}$ **then** /* increase priority */
      $\xi_i \leftarrow \xi_i + 1$;
    end
  end
  if $SoC_i \geq \mathrm{SoC}_{80\%}$ **then** /* Disconnect EV_i if charged */
    $EVSE_i \leftarrow$ available ;
    if $\xi_i \geq \xi_{max}$ **then** /* update the number of EMVs */
      $n_{EM} \leftarrow n_{EM} - 1$
    end
  end
end
solve Equation (1) /* Set the BESS priority for $V2X$ */
solve Equation (2) /* Set the BESS power limit */

Algorithm 2: Pseudo-code of the proposed supervisor.

Input: $\xi, P_{G2V}, P_{V2X}, P_{net}, P_{PV}$
Result: x
Data: m local variable
$k \leftarrow k + 1$;
Solve Equation (4) /* Calculate Photovoltaic power contribution */
Solve Equation (6c) /* Calculate grid power contribution */
Solve Equation (7) /* Find optimal solution */
for $i = 1$ **to** n **do** /* Soc update */
  Solve Equation (5)
end
Update results /* Store the results in the memory */

For real-time applications, only Section 2 will be performed, and the results will be used locally to directly control the BESS and EVs charger converter. The execution time is not a critical task for the application, and a few cycles per second are sufficient to ensure a good power balance. The linear formulation of the problem allows the code to be executed on a low-cost microcontroller.

3. Results and Discussion

The proposed supervision logic for the UFCS was numerically tested for one working day in a service area in Salerno, Italy, on the A2 motorway [49]. Statistical data were provided by ANAS, an Italian motorway observatory. The load curve, hereafter called

P_{load}, was numerically defined starting from the average data provided by TERNA in 2020 and scaled to the installed power $P_{installed} = 3$ MW, as defined for the case of study [42]. The grid load P_{load}, which is not under the control of the UFCS, is a 1.2 MW peak. The results showed that the A2 motorway circulated a mean of 39513 vehicles per day. With the hypothesis that, in the future, all vehicles will be electric, and about 0.6% stop at the service area for charging, we can assume a total of 233 refilling vehicles per day [49]. The second assumption is related to arrival time. We assumed a normal distribution with a mean of 12 am. The first two subplots of Figure 5 report the distribution and related number of EVs per hour with a time step resolution of $\Delta = 10$ min. Third, we do not have a queue; the EVs leave the charging station when all the EVSE is busy. Under these assumptions, only some EVs are charged, and only statistical considerations can be made.

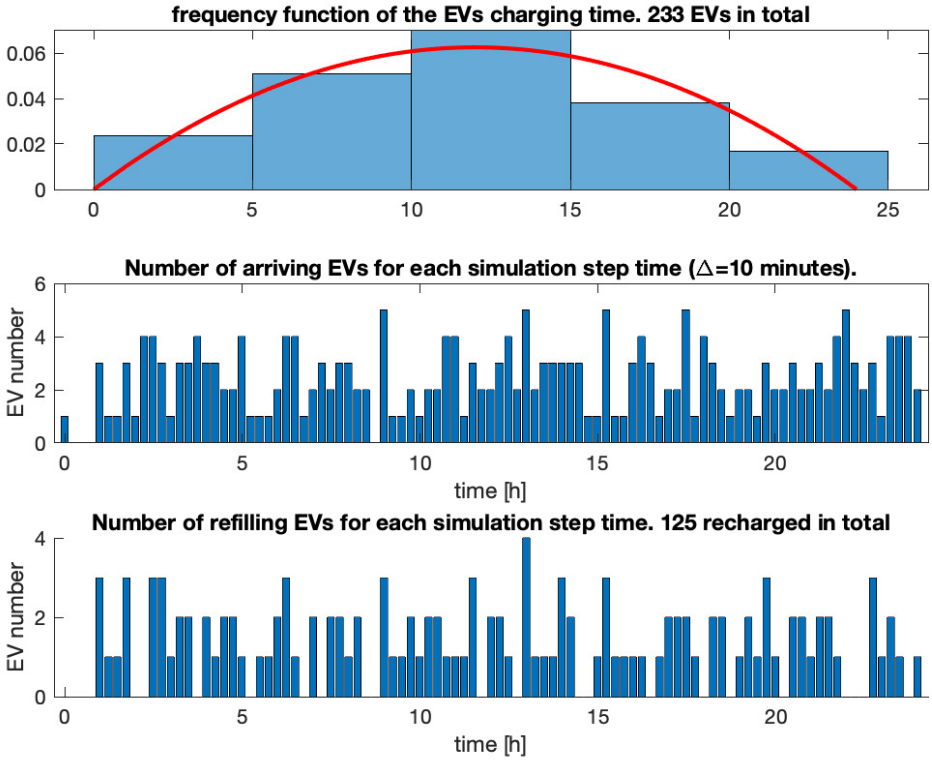

Figure 5. Normal distribution of EVs per day with hourly detail and number of uncharged vehicles.

From the UFCS as an additional power source, the UFCS has a 900 kW peak power photovoltaic plant P_{PV}. The first subplot of Figure 6 shows the maximum level of power that the UFCS can use, $P_{net} + P_{PV}$, and other relevant power used to ensure grid stability. By referring to the Figure 1 scheme, the UFCS has eight EVSE each with 800 kW peak power. The BESS' power contribution was limited to 800 kW in the charging mode and 200 kW in discharging mode, and had a storage capacity of 4 MWh. The EVs' parameters were generated as random numbers in a range similar to that defined by the market. The EVSE power is generated in the range of 400–800 kW, whereas the storage size is in the range of 225–800 kWh. All details of the simulation settings are reported in Table 1. Furthermore, the BESS is forced to help the grid in the case of the presence of EMVs, resulting in a positive effect in terms of reducing the charging time.

Table 1. Simulation setting.

Type	Value
$P_{installed}$	3 MW
P_{load}	1.2 MW peak
PV plant peak power	900 kW
EVSE maximum peak power	$random\ number \in (400, 800)$ kW
EVSE storage capacity	$random\ number \in (225, 800)$ kWh
EVSE initial *SoC*	$random\ number \in (20, 40)\%$
BESS peak charging power	800 kW
BESS peak discharging power	−200 kW
BESS storage capacity	4 MWh
BESS initial *SoC*	30%

The time step simulation is $\Delta t = 10$ min and for each sample; the supervisor acquires the working conditions and defines the storage charging/discharging power. The first subplot of Figure 6 shows that the proposed method absorbs power that is always less than or equal to $P_{net} + P_{PV}$. It is also interesting to verify that the charging and discharging priorities change in different ways. Referring to the first subplot of Figure 7, the charging priority depends on the contract, which affects the initial priority and time. The introduction of time allows the introduction of a relaxed bond for the arrival time, in contrast to FIFO methods that have the point as a hard constraint. The second subplot of Figure 7 is related to the discharging priority, and is defined by the contract as before and the *SoC*, as defined in Figure 3.

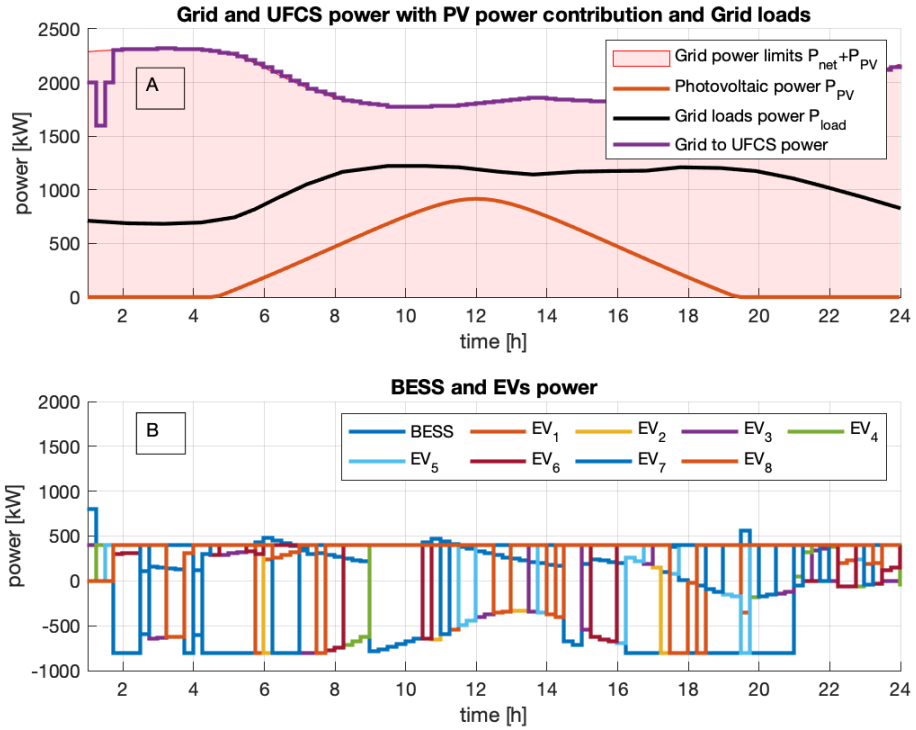

Figure 6. Subplot (**A**) shows the grid power limit, photovoltaic power contribution, and load power. The magenta colour indicates the UFCS power. Subplot (**B**) shows the details of the BESS and EVs power.

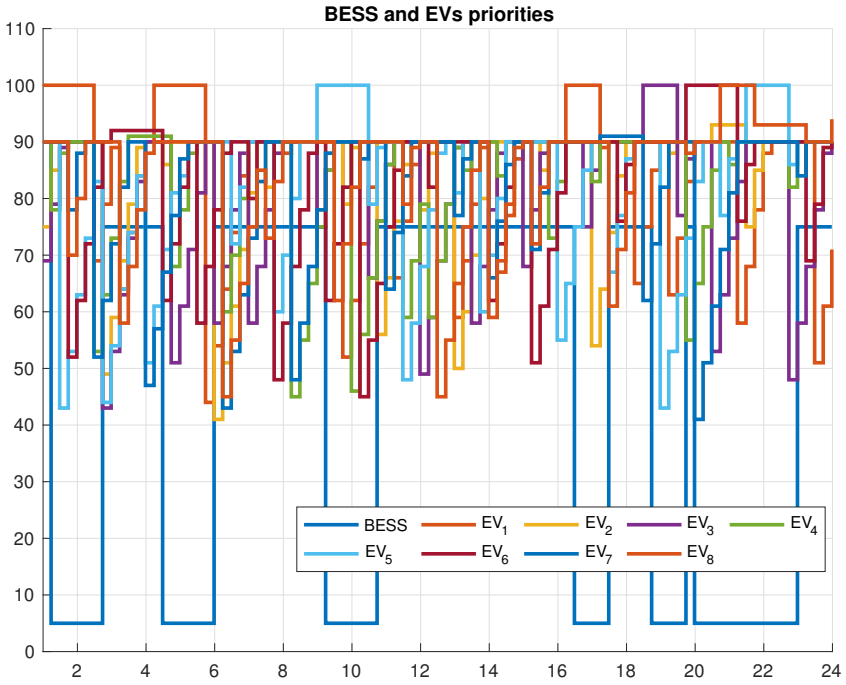

Figure 7. Charging and discharging priority.

The *SoC* as a function of time is reported in Figure 8, with a different color for each *SoC* level. We assumed red for fully discharged storage, yellow for 50%, and green for charged storage. White indicates that no EV is connected to EVSE. In the figure, the black triangle △ defines the connection time of a new EV. The BESS system was intensively used during the day, owing to the high number of EMVs (61 for the test case) managed by the UFCS. The simulations confirm the importance of the BESS and that its management is critical for improving the grid power quality and user experience in terms of reduced charging time.

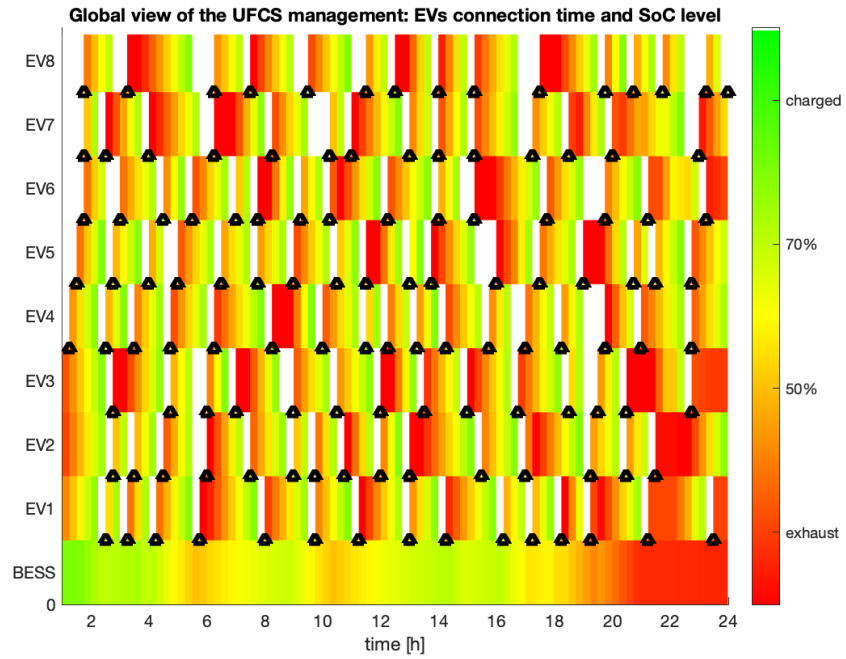

Figure 8. BESS and EVs *SoC* as a function of time. Black triangular markers are used to define the connection time.

Table 2 reports the main statistical data of the proposed method. The results indicate that the optimal charge time is 20 min, which is required to charge a vehicle with an initial *SoC* value between 30% to 80%. The worst case takes five times longer for the EMVs to complete the refiling, whereas the average charging time is about three times longer than the best case. Due to the randomly generated fleet EV, the number of stopped vehicles at the UFCS for the day changes each time the simulation is run. For the reported case study, its value was 233 stopped vehicles, with 54% vehicles charged per day. This result also depended on the number of EMVs recharged per day (38 in the case study). Performance can be improved by increasing the installed power, peak renewable power, and the number of EVSE in the UFCS. In this study, the authors have not optimized the UFCS design, focusing research interest only on the supervisory design with assigned operating conditions. Therefore, the proposed simulation software can be conveniently used to optimize the UFCS design with a defined set of input data; however, this capability was not further investigated in this study.

Table 2. Simulation results synthesis.

Type	Value
Mean charging time	47 min
Maximum charging time	1 h 40 min
Minimum charging time	20 min
Number of stopped vehicles	233
Number of refilled vehicles	125
Number of not refilled vehicles	108
Number of EMVs	38

Better performance can be achieved by increasing the installed power, including the renewable power, and increasing the peak charging power. Both new conditions can be easily considered using the proposed method by changing the simulation setting. The centralised formulation is not critical for the UFCS, but imposes a knowledge of the grid power. In a real case, P_{net} can be defined as a solution of distributed optimisation methods and passed to the proposed algorithm as an input. In this way, we have the advantages of the two methods: decentralised energy management for the grid, and respect for constraints without delays. Moreover, the UFCS is viewed by the grid as a single load. The simulative formulation of the problem allows the verification of only the formal correctness but not the capability of the system to work with a real UFCS. A formal test implies that all limits must be respected. Figure 6A clearly indicates that (7b) is always respected, because the magenta line representing the power absorbed by the UFCS is always in the pink area superior to $P_{net} + P_{PV}$. The remaining limits are shown in Figure 6B, but their graphical check is longer and expensive. The authors numerically verified the limits during the simulation, and this test was passed. It can also be observed that the mathematical correctness of the proposed method does not automatically ensure that it can operate in a real application without any changes. The method depends on inputs, and missing data or noise causes an incorrect response. Future investigations should include the introduction of noise, and a non-ideal communication channel to verify robustness. The introduction of observers can mitigate undesirable effects. The hardware-in-the-loop method is the preferred method for tests close to reality before hardware construction.

For a comparison with the state-of-the-art method, owing to differences between the proposed case of study and other relevant methods in the literature, an indirect comparison approach is adopted. In [50], the linear programming method with time-varying inequalities was compared in terms of the solution and time convergence for centralised and multi-agent smart systems. The authors showed that both methods provide the exact solution when the inputs are constant, but the multi-agent introduces a bounded tracking error in the opposite case. In addition, in terms of the solution time, centralised and decen-

tralised methods differ. The multiagent solver requires more iteration steps to reach the correct solution, whereas the centralised approach does not suffer from this problem.

In [51], the smart charging changes the duration management by differently allocating power among vehicles as a function of their state of charge and the desired end-of-charge time. The power is limited to 22 kW and the FIFO approach is adopted. Depending on the EV and the battery size, the typical charging time is between 1.5 and 3 h. This paper does not consider the grid limits as function of the time and does not introduce BESS and renewable energy to help the grid during the day, at the peak of the number of charging vehicles and the grid load. By considering these differences, the FIFO method allows us to use the charging station distribution, as in case of the considered paper, at 100% of its capability; however, the charging time is similar between vehicles.

Ref. [25] proposes dynamic programming for V2G/G2V and also integrates a renewable power source. The method introduces several charging modes: ULTRA, which is similar to our mode for EMVs, FAST, ECO, and V2G. The main difference between the proposed method and the comparison method is how the different modes are treated, which affects the scheduling order. As shown by the authors, grid limits are always respected, but the V2G vehicles are discharged up to the 50% *SoC* level, and require 22 h or more to be refilled. This approach is acceptable for urban charging stations but not for motorways, where users want to stop as little as possible. Moreover, when two or more ULTRA vehicles are connected and zero V2G vehicles are in the grid, the grid power is divided between ULTRA vehicles, thereby increasing the charging time. The work should have a similar performance to the one proposed in this work by adding a BESS with an associated V2G operating mode.

From the above comparison with the state-of-the-art method, we can conclude that the work presented here is comparable in terms of performance with the most recent case studies, but introduces some differences in terms of solution formulation and considered inputs. In particular, the introduction of priorities provides a new degree of freedom that allows the implementation of different logic, as will be required by the energy market.

4. Conclusions

In this study, a linear programming method for ultrafast charging stations is presented. This method uses priority to schedule the charging sequence and power level. In the case of sufficient power, all the EVs are charged by respecting their limits. When the available power is limited, this method reduces the absorbed power to a level acceptable for the grid. Low-priority vehicles can also be used for V2X when the grid is at its limits and high-priority vehicles are connected. The proposed ultrafast charging station integrates local storage to reduce the V2X contribution of vehicles. As tested by simulation, the proposed method never exceeded the power limits. The simulation input is numerically generated, starting from the knowledge of the statistical distribution at the location at which the ultrafast charging station is installed. The adoption of linear programming has the advantage of finding the optimal solution to the problem at each time step. This is an advantage over perturb & observe based methods, which require a longer time to find the problem solution and are critical for time-dependent systems. A drawback of this method is that it only works properly in the case of correct input data. In the case of missing or corrupted data, the solution is not optimal. It can also be noticed that the proposed ultrafast charging station behaves like a large load that slowly changes from a grid point of view. Its smooth behaviour, as confirmed by the simulation, is combined with the capability to regulate the absorbed power, improve grid power quality, and avoid grid instability conditions. The supervisor runtime code can be executed in a low-cost medium-performance microcontroller, and the charging station has costs similar to those of the independently based EVSE. By considering the benefits in terms of power quality and zero cost increase, the method can also be adopted for city-charging districts. The solution was also scalable to the desired number of EVSE. An ultrafast charging station extension can also be achieved by upgrading the basic structure, with benefits in terms of investment risks.

Author Contributions: Conceptualization, L.R.; methodology, L.R. and G.R.; software, L.R. and R.E.; validation, L.R., G.R. and R.E.; formal analysis, L.R.; investigation, L.R.; writing—original draft preparation, L.R. and G.R.; writing—review and editing, L.R., G.R. and R.E.; visualization, L.R.; supervision, L.R. All authors have read and agreed to the published version of the manuscript.

Funding: This research received no external funding.

Institutional Review Board Statement: Not applicable.

Informed Consent Statement: Not applicable.

Data Availability Statement: Data are available on request from the corresponding author.

Conflicts of Interest: The authors declare no conflict of interest.

Abbreviations

The following abbreviations are used in this manuscript:

BESS	Battery energy storage system
EMV	Emergency vehicle
EV	Electric vehicle
EVSE	Electric vehicle supply equipment
FIFO	First in, first out
G2V	Grid to vehicle
PHEV	Plug-in hybrid electric vehicle
PM	Power management
SoC	State of charge
TERNA	Italian electric power transmission *So*Ciety
UFCS	Ultrafast charging station
V2G	Vehicle-to-grid
V2X	Vehicle-to-everything

Formula Symbols

Parameters and variables:

a_i	Threshold used to decide when to stop the V2X power contribution of the ith vehicle
a_{bess}	Threshold used to decide when to stop the BESS power contribution
$Ebat_i$	Battery capacity of the ith storage
i	Index associated to the ith storage.
k	Simulation step sample
n_{EM}	Number of EMV connected to the ultrafast charging station
n_{EV}	Number of user EV connected to the ultrafast charging station
n	Number of storages including BESS, $(n = n_{EM} + n_{EV} + 1)$
N_h	Number of fleet vehicles per hour
P_{G2V}	Maximum allowed power for charging vector composed of P_i^{G2V} elements
P_{V2X}	Maximum discharging power vector composed of P_i^{V2G} elements
P_{PV}	PV power production
P_i^{EM}	Power demand of the ith EMV
P_i^{EV}	Power demand for the ith EV
P_{load}	Grid load profile
P_{net}	Power grid availability, corresponding to the peak power allowed for G2V
LT	Local time
$\overrightarrow{u}_p$	Scalar vector perpendicular to the PV panel
$\overrightarrow{\theta}(LT)$	Scalar vector position of the sun
$\xi^\top$	Priorities vector composed of ξ_i elements
$x^\top$	Optimization solution vector composed of x_i elements
Y	Constants for the conversion of irradiation into power
Δt	Step time

References

1. Kumar, M.S.; Revankar, S.T. Development scheme and key technology of an electric vehicle: An overview. *Renew. Sustain. Energy Rev.* **2017**, *70*, 1266–1285. [CrossRef]
2. Osório, G.J.; Shafie-khah, M.; Coimbra, P.D.L.; Lotfi, M.; Catalão, J.P.S. Distribution system operation with electric vehicle charging schedules and renewable energy resources. *Energies* **2018**, *11*, 3117. [CrossRef]
3. Sustainable Mobility for All. Global Roadmap of Action toward Sustainable Mobility (GRA). Available online: https://www.sum4all.org/global-roadmap-action (accessed on 23 October 2019).
4. Smith, O.; Cattell, O.; Farcot, E.; O'Dea, R.D.; Hopcraft, K.I. The effect of renewable energy incorporation on power grid stability and resilience. *Sci. Adv.* **2022**, *8*, 6734. [CrossRef] [PubMed]
5. TERNA. Storage LAB 2012–2015. 2012. Available online: https://www.terna.it/it/sistema-elettrico/innovazione-sistema/progetti-pilota-accumulo (accessed on 20 December 2022).
6. Shi, S.; Zhang, Y.; Ni, L.; Yang, Q.; Fang, C.; Wang, H.; Wang, Y.; Shi, S. Energy management method for energy storage system in PV-integrated EV charging station. In Proceedings of the 2021 IEEE International Conference on Power Electronics, Computer Applications (ICPECA), Shenyang, China, 22–24 January 2021; pp. 427–431. [CrossRef]
7. Richard, L.; Petit, M. Fast charging station with battery storage system for EV: Optimal Integration into the grid. In Proceedings of the 2018 IEEE Power & Energy *So*Ciety General Meeting (PESGM), Portland, OR, USA, 5–10 August 2018; pp. 1–5. [CrossRef]
8. E-Distribuzione. *Fotovoltaico e Superbonus 110%: Ecco Come Funziona per i Produttori Privati*; Technical Report; E-distribuzione: Sassari, Italy, 2022.
9. Parliament, I. *Law Decree 19 Maggio 2020, N. 34*; Gazzetta Ufficiale: Rome, Italy, 2020.
10. Onar, O.C.; Khaligh, A. Grid interactions and stability analysis of distribution power network with high penetration of plug-in hybrid electric vehicles. In Proceedings of the 2010 Twenty-Fifth Annual IEEE Applied Power Electronics Conference and Exposition (APEC), Palm Springs, CA, USA, 21–25 February 2010; pp. 1755–1762. [CrossRef]
11. Das, T.; Aliprantis, D.C. Small-signal stability analysis of power system integrated with PHEVs. In Proceedings of the 2008 IEEE Energy 2030 Conference, Atlanta, GA, USA, 17–18 November 2008; pp. 1–4. [CrossRef]
12. Bañol Arias, N.; Hashemi, S.; Andersen, P.B.; Træholt, C.; Romero, R. Distribution system services provided by electric vehicles: Recent status, challenges, and future prospects. *IEEE Trans. Intell. Transp. Syst.* **2019**, *20*, 4277–4296. [CrossRef]
13. Agency, E.E. *Electric Vehicles in Europe. European Environmental Agency*; Technical Report Report No. 20/2016; Publications Office of the European Union: Brussels, Belgium, 2016.
14. Chandra Mouli, G.R.; Kefayati, M.; Baldick, R.; Bauer, P. Integrated PV charging of EV fleet based on energy prices, V2G, and offer of reserves. *IEEE Trans. Smart Grid* **2019**, *10*, 1313–1325. [CrossRef]
15. Rubino, L.; Capasso, C.; Veneri, O. Review on plug-in electric vehicle charging architectures integrated with distributed energy sources for sustainable mobility. *Appl. Energy* **2017**, *207*, 438–464. [CrossRef]
16. Ghazanfari, A.; Perreault, C. The path to a Vehicle-to-Grid future: Powering electric mobility forward. *IEEE Ind. Electron. Mag.* **2022**, *16*, 4–13. [CrossRef]
17. Yan, J.; Xu, G.; Qian, H.; Xu, Y. Battery fast charging strategy based on model predictive control. In Proceedings of the 2010 IEEE 72nd Vehicular Technology Conference–Fall, Ottawa, ON, Canada, 6–9 September 2010; pp. 1–8. [CrossRef]
18. Alliance, O.C. Open Charge Protocol 201. Techreport. April 2018. Available online: https://www.openchargealliance.org/protocols/ocpp-201/ (accessed on 20 December 2022).
19. Suhail, H.S.; Selim, U.T.; Akhtar, K. A review of IEC 62351 security mechanisms for IEC 61850 message exchanges. *IEEE Trans. Ind. Inform.* **2019**, *16*, 5643–5654. [CrossRef]
20. *ISO 15118-1:2019*; Road Vehicles–Vehicle to Grid Communication Interface–Part 1: General Information and Use Case Definition; Technical Report; International Electrotechnical Commission (IEC): Geneva, Switzerland, 2019.
21. *IEC 61851-24:2014*; Electric Vehicle Conductive Charging System–Part 24: Digital Communication between a d.c. EV Charging Station and an Electric Vehicle for Control of d.c. Charging; Technical Report; International Electrotechnical Commission (IEC): Geneva, Switzerland, 2014.
22. Abdalzaher, M.S.; Fouda, M.M.; Ibrahem, M.I. Data privacy preservation and security in smart metering systems. *Energies* **2022**, *15*, 7419. [CrossRef]
23. Elwekeil, M.; Abdalzaher, M.S.; Seddik, K. Prolonging smart grid network lifetime through optimising number of sensor nodes and packet length. *IET Commun.* **2019**, *13*, 2478–2484. [CrossRef]
24. Abdalzaher, M.S.; Salim, M.M.; Elsayed, H.A.; Fouda, M.M. Machine learning benchmarking for secured IoT smart systems. In Proceedings of the 2022 IEEE International Conference on Internet of Things and Intelligence Systems (IoTaIS), Bali, Indonesia, 24–26 November 2022; pp. 50–56. [CrossRef]
25. Salvatti, G.A.; Carati, E.G.; Cardoso, R.; da Costa, J.P.; Stein, C.M.d.O. Electric vehicles energy management with V2G/G2V multifactor optimization of smart grids. *Energies* **2020**, *13*, 1191. [CrossRef]
26. Wu, Y.; Ravey, A.; Chrenko, D.; Miraoui, A. A real time energy management for ev charging station integrated with local generations and energy storage system. In Proceedings of the 2018 IEEE Transportation Electrification Conference and Expo (ITEC), Long Beach, CA, USA, 13–15 June 2018; pp. 1–6. [CrossRef]

27. Melhem, F.Y.; Grunder, O.; Hammoudan, Z.; Moubayed, N. Optimization and energy management in smart home considering photovoltaic, wind, and battery storage system with integration of electric vehicles. *Can. J. Electr. Comput. Eng.* **2017**, *40*, 128–138. [CrossRef]
28. van der Meer, D.; Chandra Mouli, G.R.; Morales-España Mouli, G.; Elizondo, L.R.; Bauer, P. Energy management system with PV power forecast to optimally charge EVs at the workplace. *IEEE Trans. Ind. Inform.* **2018**, *14*, 311–320. [CrossRef]
29. ABB. *Optimized Energy Management for Electric Vehicle Chargers–EVSS Control 100*; Technical Report; ABB: Delft, The Netherlands, 2021.
30. DELTA. *DeltaGrid EVM*; Technical Report; Delta Electronics: Taipei City, Taiwan, 2022.
31. SHELL. *Ultra-Fast Chargers Enabled by Our Energy Management Solutions*; Technical Report; SHELL: London, UK, 2022.
32. TERNA. *Pilot Storage Projects*; Technical Report; Driving Energy: Rome, Italy, 2015.
33. TERNA. *Development Plan*; Technical Report; Driving Energy: Rome, Italy, 2020.
34. Varghese, S.S.; Joos, G.; Ali, S.Q. Load management strategy for DC fast charging stations. In Proceedings of the 2021 IEEE Energy Conversion Congress and Exposition (ECCE), Vancouver, BC, Canada, 10–14 October 2021; pp. 1620–1626. [CrossRef]
35. Bhuiyan, E.A.; Hossain, M.Z.; Muyeen, S.; Fahim, S.R.; Sarker, S.K.; Das, S.K. Towards next generation virtual power plant: Technology review and frameworks. *Renew. Sustain. Energy Rev.* **2021**, *150*, 111358. [CrossRef]
36. Hu, J.; Saleem, A.; You, S.; Nordström, L.; Lind, M.; Østergaard, J. A multi-agent system for distribution grid congestion management with electric vehicles. *Eng. Appl. Artif. Intell.* **2015**, *38*, 45–58. [CrossRef]
37. Tan, X.; Li, Q.; Wang, H. Advances and trends of energy storage technology in microgrid. *Int. J. Electr. Power Energy Syst.* **2013**, *44*, 179–191. [CrossRef]
38. Laureri, F.; Puliga, L.; Robba, M.; Delfino, F.; Bulto, G.O. An optimization model for the integration of electric vehicles and smart grids: Problem definition and experimental validation. In Proceedings of the 2016 IEEE International Smart Cities Conference (ISC2), Trento, Italy, 12–15 September 2016; pp. 1–6. [CrossRef]
39. Khalid, H.M.; Flitti, F.; Muyeen, S.M.; Elmoursi, M.S.; Sweidan, T.O.; Yu, X. Parameter estimation of vehicle batteries in V2G systems: An exogenous function-based approach. *IEEE Trans. Ind. Electron.* **2022**, *69*, 9535–9546. [CrossRef]
40. Khalid, H.M.; Peng, J.C.H. Bidirectional charging in V2G systems: An in-cell variation analysis of vehicle batteries. *IEEE Syst. J.* **2020**, *14*, 3665–3675. [CrossRef]
41. Khalid, H.M.; Ahmed, Q.; Peng, J.C.H.; Rizzoni, G. Current-split estimation in Li-Ion battery pack: An enhanced weighted recursive filter method. *IEEE Trans. Transp. Electrif.* **2015**, *1*, 402–412. [CrossRef]
42. TERNA. *Annual Report*; Technical Report; TERNA: Rome, Italy, 2020.
43. TERNA. *Renewable Sources*; Technical Report; TERNA: Rome, Italy, 2022.
44. Perpiñan, O.; Lorenzo, E.; Castro, M. On the calculation of energy produced by a PV grid-connected system. *Prog. Photovolt. Res. Appl.* **2007**, *15*, 265–274. [CrossRef]
45. Almonacid, F.; Rus, C.; Pérez, P.; Hontoria, L. Estimation of the energy of a PV generator using artificial neural network. *Renew. Energy* **2009**, *34*, 2743–2750. [CrossRef]
46. Aste, N.; Pero, C.D.; Leonforte, F.; Manfren, M. A simplified model for the estimation of energy production of PV systems. *Energy* **2013**, *59*, 503–512. [CrossRef]
47. Capasso, C.; Rubino, L.; Rubino, G.; Veneri, O. Data analytics for performance modelling of photovoltaic systems in the internet of energy scenario. In Proceedings of the 2021 IEEE 15th International Conference on Compatibility, Power Electronics and Power Engineering (CPE-POWERENG), Florence, Italy, 14–16 July 2021; pp. 1–6. [CrossRef]
48. Zine, B.; Bia, H.; Benmouna, A.; Becherif, M.; Iqbal, M. Experimentally validated coulomb counting method for battery state-of-charge estimation under variable current profiles. *Energies* **2022**, *15*, 8172. [CrossRef]
49. ANAS. ANAS Strade. Available online: https://www.stradeanas.it/en (accessed on 20 December 2022).
50. Hosseinzadeh, M.; Garone, E.; Schenato, L. A distributed method for linear programming problems with box constraints and time-varying inequalities. *IEEE Control Syst. Lett.* **2019**, *3*, 404–409. [CrossRef]
51. Lo Franco, F.; Cirimele, V.; Ricco, M.; Monteiro, V.; Afonso, J.L.; Grandi, G. Smart charging for electric car-sharing fleets based on charging duration forecasting and planning. *Sustainability* **2022**, *14*, 12077. [CrossRef]